IEEE Access
Multidisciplinary | Rapid Review | Open Access Journal

Received August 4, 2021, accepted August 24, 2021, date of publication September 16, 2021, date of current version September 27, 2021.

Digital Object Identifier 10.1109/ACCESS.2021.3113325

Analysis of Spatial Vibration on Scanning Mirror Imaging Based on Frequency Filtering

ZIQI YU, LI JIANG, AND ZHIHAI YAO
College of Science, Changchun University of Science and Technology, Changchun 130022, China
Corresponding author: Li Jiang (jiangli@cust.edu.cn)

This work was supported by the National Natural Science Foundation of China (NSFC) under Grant 62101071 and Grant 62171430.

ABSTRACT In order to analyze the impact of multisource vibration on the imaging quality of aerospace optical payload during camera scanning, a dynamic imaging quality degradation model fused with satellite vibration filter templates is established. Firstly, according to the motion scanning process of the TDI camera, a filter template combining the amplitude and frequency of the vibration source is designed; Secondly, a piecewise function of satellite vibration with a frequency range of 1 Hz to 1000 Hz is obtained by curve fitting, and the amplitudes of different frequency ranges are brought into the image filter template to simulate the output image affected by the vibration. Finally, the output degraded image is analyzed through structural similarity and mean square error. The simulation results show that during the imaging process of the aerospace scanning mirror, the line frequency of the camera changes regularly with the scanning speed. When platform vibration frequency is similar to the camera's exposure frequency, it will have a large impact on image quality. Therefore, when the camera's exposure frequency is 110 Hz, vibration at a frequency of 110 Hz will further degrade the image quality. This article is expected to provide guidance for spatial vibration suppression and image quality degradation assessment in the imaging process of aerospace scanning mirrors.

INDEX TERMS Frequency filtering, spatial vibration, scan imaging, frequency and amplitude.

I. INTRODUCTION

Aerospace optical payloads can realize detailed or rough imaging of the earth scenery without national boundaries in space, thereby performing overall situational awareness in a large area or the identification of fine targets between ground objects, which plays an important role in national economic construction and national defense [1]–[3]. Limited by the constraints between the aperture and focal length of the traditional optical system, the space-based optical payload cannot achieve high-resolution and large-width imaging at the same time in the traditional push-broom imaging mode [4]–[6]. In recent years, scholars have successively proposed space-based optical system swing mirror scanning technology and push-frame imaging technology to solve the constraints between the aperture and focal length [7]–[9], which makes high-resolution large-width imaging technology possible. However, this complex and cooperative dynamic scanning imaging mode also has new spatial disturbance factors, which brings new challenges to high-quality scanning imaging. Therefore, it is necessary to analyze the impact of the spatial disturbance of the space-based scanning imaging mode on the image quality.

In order to analyze the impact of platform vibration on payloads imaging, scholars mainly analyzed characteristics of different types of spatial vibration and the impact on imaging quality [10]–[12]. For the characteristics of spatial disturbance, Japan ETS-VI Satellite Test Center [13] used laser communication technology to test the characteristics of the platform vibration, and found that the power spectral density of different satellites had similar regularity, which was the superimposition of continuously declining spectrum and multiple resonance peaks. As the vibration frequency increased, the amplitude decreased gradually. O. Adar, N. S. Kopeika and others [14] derived the high and low frequency vibration transfer functions based on the frequency domain and time domain. These formulas are universally applicable to spatial vibration. Chen [15] proposed a double isolation system, and took flywheel micro-vibration as an example, analyzed the decay time of flywheel spiral effect, and proved that the system could improve the attenuation rate of high frequency vibration; Wang [16] divided the platform

The associate editor coordinating the review of this manuscript and approving it for publication was Chao Zuo.

vibration into linear vibration, sinusoidal vibration and random vibration according to the vibration characteristics, and took sinusoidal vibration as an example to study the impact of vibration parameters such as vibration frequency, amplitude and phase on image quality. Wei [17] of Harbin Institute of Technology divided the space-based imaging process into several ideal simulation subsystem links, such as atmospheric links, detectors and platform motion, and designed a full-link imaging system to further discuss the impact of vibration on the imaging systems.

The application scenarios mentioned above for analyzing spatial vibration are all in the classic on-orbit push-broom imaging mode. The type of vibration is limited to components such as flywheels and solar arrays. The frequency and amplitude of vibration are also limited to the range of traditional integration level and exposure time; With the development of space-based scanning mirror imaging technology, the dependence on dynamic scanning components has increased, and new spatial disturbances have appeared. Therefore, it is necessary to summarize the vibration characteristics related to dynamic imaging and analyze the law of image quality degradation in dynamic imaging mode.

Based on the theory of space-based payload scanning mirror imaging, this paper establishes the motion imaging equation of TDI camera, sorts out the types and characteristics of spatial vibration, and integrates the filter template of vibration source amplitude and frequency in the image quality degradation model of dynamic imaging. It is expected to analyze the image quality degradation phenomenon caused by vibration in the process of the space-based dynamic scanning mirror imaging.

II. MATHEMATICAL MODEL OF SPACE IMAGING

Space-based scanning mirror imaging technology does not change the satellite detector and optical system parameters. While the satellite is flying on-orbit, it uses the pointing accuracy control technology of the scanning mechanism to perform swing mirror scanning in any direction. The camera combines push-broom imaging of the payload along the orbital direction and scanning imaging in the vertical orbital direction, which broadens the detection range of the camera on the ground. Fig. 1 shows the dynamic imaging process of the scanning mirror system. When the payload scans the sub-satellite point, the satellite attitude angle is small, and the target position will slightly deviate from the actual position. The output image is similar to the classic push-broom image, as shown in Fig. 1-①. When the attitude angle of the satellite scanning is large, due to the influence of the curvature of the earth, the ground track of the scanned single frame is approximately trapezoidal, and the overall image is a concave quadrilateral image with wider sides in the vertical track direction, as shown in Fig. 1-②. There are multiple spatial vibrations during dynamic scanning, and the frequency and amplitude of the vibration directly affect the imaging payload, resulting in multilevel cumulative crosstalk in TDI imaging, which means that there will be a certain frequency of pulse influence during the load working process. The output image is distorted and degraded as shown in Fig. 1-③.

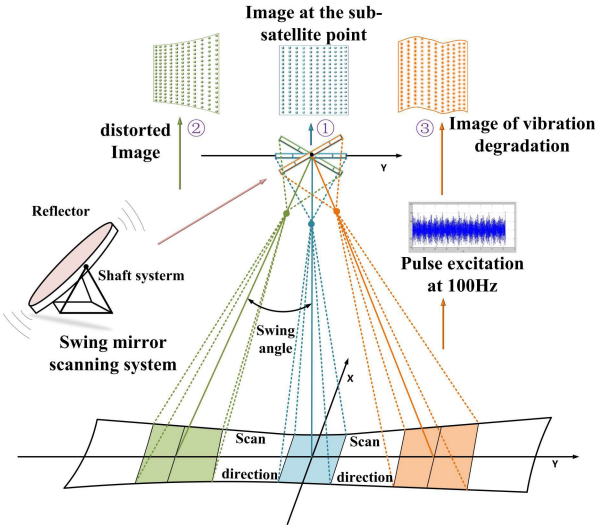

FIGURE 1. Schematic diagram of space-based scanning mirror imaging with fusion space vibration.

A. VIBRATION IMAGING MODEL OF SPACE-BASED SCANNING MIRROR

In order to simulate the process of imaging the ground scene by the space-based optical payload, it is necessary to use the ray tracing method to determine the curvature mapping relationship between each pixel in the image plane and the ground scene point. Scanning motion and spatial vibration process need to be simulated, in order to accurately project the ground scene image $G(x, y)$ to the camera focal plane $I_f(x, y)$, the ground scene curvature equation $T\{G(x, y)\}$ is established firstly, then Fourier transform and spatial vibration filtering are performed to generate a Fourier spectrum image $F(u, v)$, as shown in (1). At last, the Fourier spectrum image is subjected to inverse Fourier transform to obtain the camera focal plane image $I_f(x, y)$, as shown in (2), the flow chart of space-based payload scanning mirror imaging is shown in Fig. 2.

$$F(u, v) = \left| \iint h(s_x, s_y)\, e^{-j2\pi(us_x + vs_y)} ds_x ds_y \right| \cdot \sum_{x=0}^{M-1} \sum_{y=0}^{N-1} T\{G(x, y)\} e^{-j2\pi(ux/M + vy/N)} \quad (1)$$

In the (1):

$F(u, v)$ − The frequency spectrum image obtained by the filtering process of the original image after Fourier transform;

$h(s_x, s_y)$ − The point spread function caused by vibration, represent the actual physical distance of each image pixel;

f_x, f_y − Coordinates of the filter template;

M, N − The output image size of the camera focal plane;

$G(x, y)$ − Ground image;

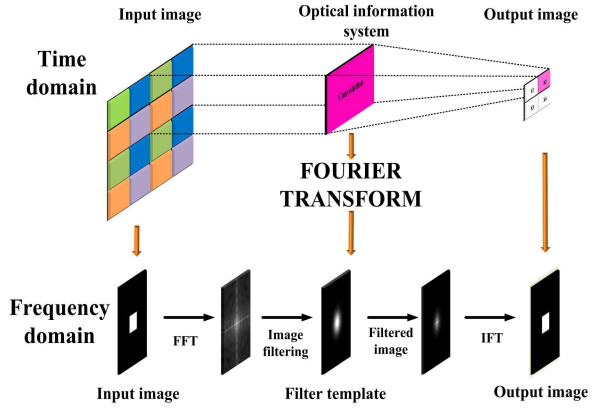

FIGURE 2. Chart of space vibration imaging model for space-based payload scanning.

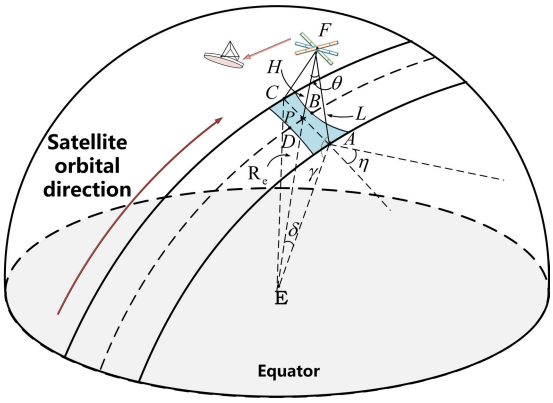

FIGURE 3. Schematic diagram of the scanning light imaged by the scanning mirror pointing along with the movement.

$T\{G(x,y)\}-$ Geometric transformation process of ground image based on ray tracing.

$$I_f(x,y)=\frac{1}{MN}\sum_{u=0}^{M-1}\sum_{v=0}^{N-1}F(u,v)e^{j2\pi(ux/M+vy/N)} \quad (2)$$

In the (2):

$I_f(x,y)-$ Final degraded image;

$u=0,1,2,3,\ldots,M-1; v=0,1,2,3,\ldots,N-1-$ Same size as the matrix of the input image.

B. CURVATURE MAPPING FUNCTION BASED ON SCANNING MOTION EQUATION

The ground scene is mapped into a two-dimensional image, where the x and y directions of the pixel determine the camera attitude angle and corresponding curvature changes. The attitude angle is solved by the scanning speed and time, and the corresponding curvature distortion is determined by the distance between the object and the image and the radius of curvature of the earth. Therefore, the curvature mapping equation of the ground scene is:

$$T[x,y]=M\{R_e,\omega,l,t,f,a\}\times G[x,y] \quad (3)$$

In the (3):

R_e — Earth radius length;

ω — Spin velocity of payload;

l — Length of objective distance;

t — Time of camera scanning (The sub-satellite point is the initial moment);

f — Focus of camera;

a — pixel size.

The angle change of the imaging light with the change in the direction of the scanning mirror is the essence of the imaging process. When the sub-satellite point is the initial zero phase of the scanning mirror motion, the attitude angle after the time t is θ, $\theta=\omega\times t$, with the geocentric angle δ and the projection angle η change simultaneously. As shown in Fig. 3, the earth's radius is R_e and the orbital height is H, the $\angle FAE$ can be calculated by the law of sines, then according to the principle of geometric triangle, η and the can be calculated by the following formula:

$$\eta=\pi-\arctan\left(\frac{R_e+H}{R_e}\cdot\sin(\theta(t))\right)$$
$$\delta=\pi-\left[\theta(t)+\arcsin\left(\frac{R_e+H}{R_e}\cdot\sin(\theta(t))\right)\right] \quad (4)$$

in the (4): $\theta(t)$ is the periodic function of the camera scanning angle. The result shows that within the effective scanning angle range of the swing mirror, as the attitude angle θ increases, the geocentric angle δ and the projection angle η increase simultaneously, and the corresponding object distance l and ground resolution A_C also need to be recalculated.

$$l=\left[H^2+2R_e(1+H)(1-\cos\delta)\right]^{1/2}$$
$$A_C=\frac{l\times a}{f\times\cos\eta} \quad (5)$$

According to the calculation result of the object distance l in (5), combined with the satellite on-orbit speed $v_t=\mu/(R_e+H)$ (μ is the gravitational constant), the resultant velocity $V_{compose}$ of the push-broom camera on the ground can be obtained. The formula is as follows:

$$V_{compose}=\left[(\omega l)^2+(v_t)^2\right]^{1/2} \quad (6)$$

From the line frequency definition formula $F_q=V_{compose}/A_C$ of the camera scan, it can be seen that the camera line frequency is the quotient of the camera's sweeping speed on the ground and the ground resolution. The (5) and (6) are brought into the line frequency definition formula, which is obtained as follows (7), as shown at the bottom of the next page, then the interline transfer time Δt could be expressed as:

$$\Delta t=\frac{1}{F_q} \quad (8)$$

Assuming that the number of imaging levels from the sub-star point to the pointing position of the ray is N, and

further solving (8), the imaging time t of scanning imaging is obtained:

$$t = \sum_{1}^{N} \Delta t \tag{9}$$

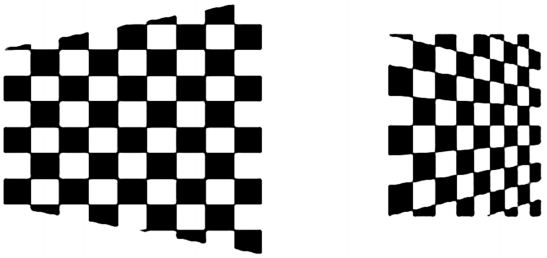

(a) (b)

FIGURE 4. Distorted image. (a) Schematic diagram of ground imaging area. (b) Schematic diagram of imaging where the object image is mapped to the focal plane.

In the scanning mirror imaging process, the plane mirror, shaft system and motor drive system are regarded as a whole swing mirror scanning system. The actual ground imaging area is an approximate isosceles trapezoid, therefore, there is an imaging distortion effect as shown in Fig.4 in the actual imaging result. The image output process from the ground image 4-(a) to the camera focal plane 4-(b) is simulated by establishing the operational relationship between the ground image and the camera focal plane. According to the invariance of the field of view of the imaging system, the conversion relationship between the object plane and the focal plane is established, and the focal plane coordinate system $I(x, y)$ is established with the camera center as the coordinate origin O. Then the field of view relationship at any point $I\left(I_{xi}, I_{yi}\right)$ on the focal plane is:

$$\begin{cases} \alpha = \arctan\left(\dfrac{I_{xi} \times a}{f}\right) \\ \beta = \arctan\left(\dfrac{I_{yi} \times a}{f}\right) \end{cases} \tag{10}$$

in the formula: α is the field angle of the pixel point along satellite flight path track; β is the field angle of the pixel point perpendicular to the satellite flight path track; f is the camera focal length. In the same way, the ground coordinate system $G(x, y)$ is established with the intersection of the optical axis and the ground as the center point P, and any point $G\left(G_{x_i}, G_{y_i}\right)$ on the object plane can be expressed as:

$$\begin{cases} G_{xi} = \dfrac{H}{\cos(\theta(t) + \beta)} \cdot \tan(\alpha) \\ G_{yi} = H \cdot \tan(\theta(t) + \beta) \end{cases} \tag{11}$$

Substituting (10) into (11), the mathematical relationship between focal plane coordinates and ground coordinates can be obtained as:

$$\begin{aligned} G_{xi} &= \frac{H}{\cos\left(\theta(t) + \arctan\left(\frac{I_{yi} \times a}{f}\right)\right)} \cdot \frac{I_{xi} \times a}{f} \\ G_{yi} &= H \cdot \tan\left(\theta(t) + \arctan\left(\frac{I_{yi} \times a}{f}\right)\right) \end{aligned} \tag{12}$$

(12) is the transformation process between the ground coordinate system $G(x, y)$ and the focal plane coordinate system $I(x, y)$, expressed as a generalized function $T\{\}$:

$$I(x, y) = T\{G(x, y)\} \tag{13}$$

C. INVERSION TRANSFORMATION BETWEEN OBJECTS AND IMAGES BASED ON SPATIAL VIBRATION FILTERING TECHNOLOGY

In the process of scanning mirror imaging, in addition to the distortion of the output image, the vibration of the platform will also lead the image plane to shake regularly, which will cause the output image to become blurred and reduce the image quality. This kind of vibration of a certain frequency has limitations when calculating in the time domain. If the vibration frequency is high, it will be difficult to reproduce the image degradation phenomenon through the convolution calculation method in the time domain, therefore, the impact of this vibration on image quality can be transformed into the frequency domain for evaluation. Set the image of the camera focal plane as $I(x, y)$, and the point spread function generated by the vibration as $h\left(s_x, s_y\right)$. According to the principle of image filtering, it can be known that the degraded image $I_f(x, y)$ is the convolution result of the image $I(x, y)$ of the camera focal plane and the point spread function $h\left(s_x, s_y\right)$, so:

$$I_f(x, y) = I(x, y) * h\left(s_x, s_y\right) \tag{14}$$

let each term in the above formula be used as the Fourier transform input term $f(x, y)$ to get the output result $P(u, v)$:

$$P(u, v) = \sum_{x=0}^{M-1} \sum_{y=0}^{N-1} f(x, y) \mathrm{e}^{-j2\pi\left(\frac{ux}{M} + \frac{vy}{N}\right)} \tag{15}$$

(14) is transformed into the frequency domain by (15), which can be expressed as:

$$F(u, v) = K(u, v) H(u, v) \tag{16}$$

in the formula, $K(u, v)$ is the input image frequency spectrum; $F(u, v)$ is the output image frequency spectrum; $H(u, v)$ is the Fourier transform result of the point spread function caused by vibration, which is called the transfer

$$F_q = \frac{f \cdot \cos\eta \cdot \sqrt{\omega^2\left(H^2 + 2R_e(1 + H)(1 - \cos\delta)\right) + \mu/(\mathrm{Re} + H)}}{a \cdot \sqrt{H^2 + 2R_e(1 + H)(1 - \cos\delta)}} \tag{7}$$

function. Generally, $MTF(v) = F(v)_{output}/F(v)_{input}$ is used to represent the physical meaning of the transfer function, v is the spatial frequency, $F(v)_{input}$ is the input image frequency spectrum, and $F(v)_{output}$ is the output image frequency spectrum.

Therefore, the known transfer function can be used to invert the degradation process of high quality images disturbed by vibration. The focal plane displacement is a key parameter to derive the transfer function caused by vibration. The angle between the optical axis of the payload disturbed by the vibration and the original optical axis is called the displacement angle, and the focal plane displacement D could be calculated by the displacement angle σ and the focal length f:

$$D = f \cdot \tan(\sigma) \tag{17}$$

In the process of low frequency vibration, the camera exposure time is less than the platform vibration period, so the periodic vibration cannot be completed within the limited exposure time. The equivalent displacement d_{avg} of the focal plane is a periodic function of the camera exposure time t_e and vibration period T:

$$d_{\text{avg}} = \left| 2D\cos\left[\frac{2\pi}{T}\left(\frac{T}{4} - \frac{t}{2}\right)\right]\right| \tag{18}$$

Substituting the focal plane displacement caused by the vibration in the high and low frequency range into the following transfer function formula, the transfer function in the full frequency range can be obtained:

$$\begin{aligned} MTF(v) &= \mathrm{J}_0(2\pi v D) \quad (t \geq T) \\ MTF(v) &= \operatorname{sinc}(\pi d_{avg} v) \quad (t < T) \end{aligned} \tag{19}$$

in the formula: $\mathrm{J}_0()$ is the 0-order Bessel function; and sinc () is the sinc function.

The transfer function expression (19) is substituted into the (16) to obtain the frequency spectrum $F(u, v)$ of the output image, the Fourier inversion result of the frequency spectrum image is the degraded image $I_f(x, y)$ disturbed by the vibration of the platform:

$$I_f(x, y) = \frac{1}{MN}\sum_{u=0}^{M-1}\sum_{v=0}^{N-1} F(u, v)\mathrm{e}^{j2\pi(ux/M + vy/N)} \tag{20}$$

D. INVERSION IMAGE QUALITY ASSESSMENT

The differences in image degradation can be directly observed by subjective evaluation method and also objectively evaluated by both mean square error (MSE) and structural similarity (SSIM) functions called by MATLAB. The formula of mean square error (MSE) is:

$$MSE = \frac{1}{MN}\sum_{x=1}^{M}\sum_{y=1}^{N}\left[I(x_i, y_i) - I_f(x_i, y_i)\right]^2 \tag{21}$$

In the formula, $I(x_i, y_i)$ and $I_f(x_i, y_i)$ are the pixel values of the reference image and the evaluated image at (x_i, y_i); M and N are also the image size. The mean square error value approaching 0 indicates that the image quality is good. The formula for structural similarity (SSIM) is:

$$SSIM(x_i, y_i) = [l(x_i, y_i)]^{\tau 1}[c(x_i, y_i)]^{\tau 2}[s(x_i, y_i)]^{\tau 3} \tag{22}$$

In the formula, $[l(x_i, y_i)]^{\tau 1}$ is brightness distortion; $[c(x_i, y_i)]^{\tau 2}$ is contrast distortion; $[s(x_i, y_i)]^{\tau 3}$ is structural distortion. $\tau 1, \tau 2$ and $\tau 3$ are the corresponding weight coefficients respectively. The structural similarity value approaching 1 indicates that the image similarity and sharpness are high. The degree of image distortion can be evaluated by the above subjective and objective methods.

III. IMAGE SIMULATION AND ANALYSIS

A. DESIGN OF SIMULATION MODEL DATA

According to the above theory, it is necessary to further analyze the impact of the platform vibration of the dynamic scanning mirror imaging mode on the output image through simulation, and use the mean square error, structural similarity and transfer function as the image quality evaluation indicators. The orbit height is set to 500km, the earth radius is set to 6371km, the camera focal length is set to 0.5m, and the pixel size is set to 3.5μm. During the dynamic imaging process, the camera mirror swings 1° every 100ms on average. This continuous periodic spin scan motion will cause the camera line frequency and exposure time to change.

1) CHANGES IN CAMERA PARAMETERS

During the dynamic scanning imaging process, the attitude angles $\theta(t)$ corresponding to each single frame of exposure image are all different. Because the attitude angle of the payload determines the efficiency of ground push-broom imaging, the camera will adjust its line frequency and exposure time to meet the synchronization with the ground push-broom efficiency. By (4) to (9), the function curve of camera exposure time and frequency with a camera swing angle of 0°∼50° as shown in Fig. 5 can be obtained:

It can be seen from Fig.5 that the absolute value of the slope of the camera's exposure function curve increases with the increase of the attitude angle. The dynamic scanning movement of the camera will change the exposure time of the camera, which is different from the traditional vibration interference imaging analysis. In order to intuitively compare the difference of image degradation in different attitude angle models, instantaneous imaging models with attitude angles of 0°, 15°, 30°, 40°, 45°, 50° are established through unequal interval sampling, then the image degradation process was inverted. The exposure time and frequency corresponding to the above models are sorted out as shown in Table 1:

2) DATA ANALYSIS OF SPACE PLATFORM VIBRATION

It is necessary to know the regularity of platform vibration in the whole frequency rang to analyze the impact of vibration on the output image of the payload during the dynamic scanning mirror imaging process. Fig.6 shows the satellite power spectral density image [13].

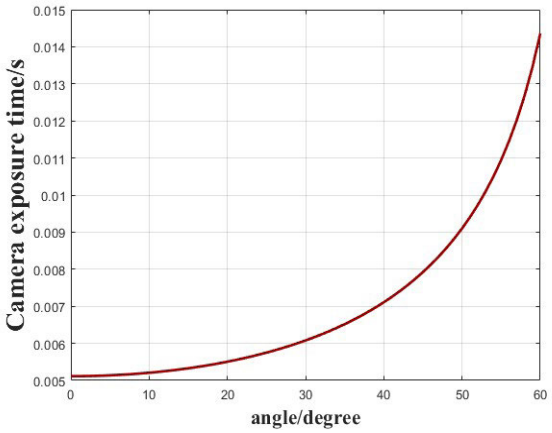

(a)

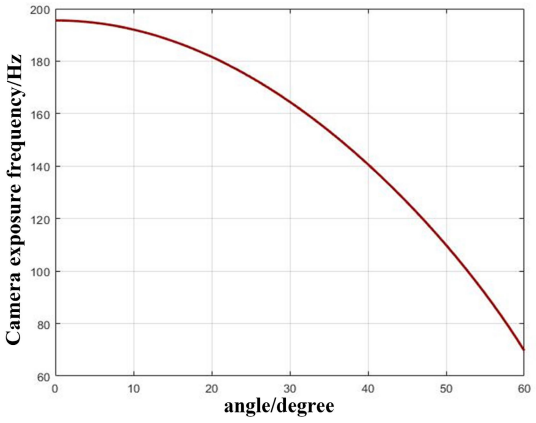

(b)

FIGURE 5. The image of the camera parameters changing with the swing angle. (a)Schematic diagram of changes in camera exposure time; (b)Schematic diagram of changes in camera exposure frequency.

TABLE 1. Dynamic parameters of the TDI camera.

Attitude angle	Camera exposure time	Frequency
0°	0.0051s	196Hz
15°	0.0053s	188 Hz
30°	0.0061s	164 Hz
40°	0.0071s	141 Hz
45°	0.0079s	126 Hz
50°	0.0091s	110 Hz

A conclusion can be known by analyzing Fig. 6 that the frequency and amplitude of the satellite platform vibration are correlated, and the satellite will produce vibrations with different levels of amplitude in different frequency ranges. The vibration frequency below 2Hz is generated by the coupling of multiple components of the payload, and the amplitude reaches more than 70 arc-seconds (330μrad). As the vibration frequency of the platform increases, the vibration amplitude gradually decreases. When the frequency increases to 100Hz∼1000Hz, the amplitude even drops to 0.1μrad. The above data shows that the platform vibration amplitude has a large difference in different frequency

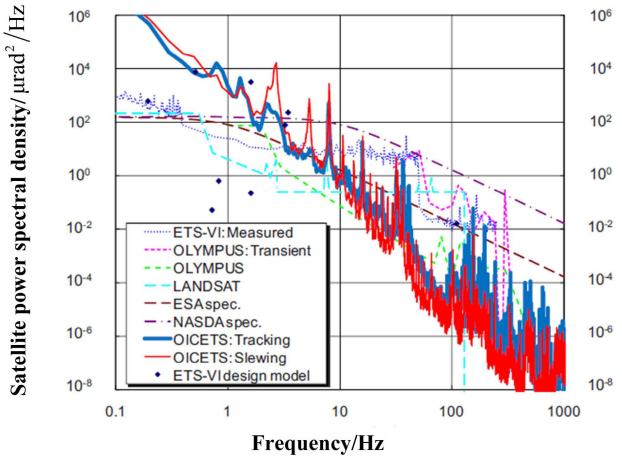

FIGURE 6. Power spectral density of satellite.

ranges [18], [19]. In order to explore the law of the image quality degradation caused by the actual vibration of the payload, a functional image with the satellite vibration frequency as the independent variable and the displacement angle as the dependent variable will be illustrated. Figure 7 shows the derivation process of the piecewise function. The satellite data is sampled in the equal frequency interval. However, the coordinates of the sampled point (x, y) do not represent the physical meaning of the study in the dynamic model. The research variables (x, σ) can be calculated by the coordinate transformation of the point (x, y), In order to avoid the errors caused by under-fitting and over-fitting, the discrete points (x, σ) are fitted to a piecewise function by the least square method.

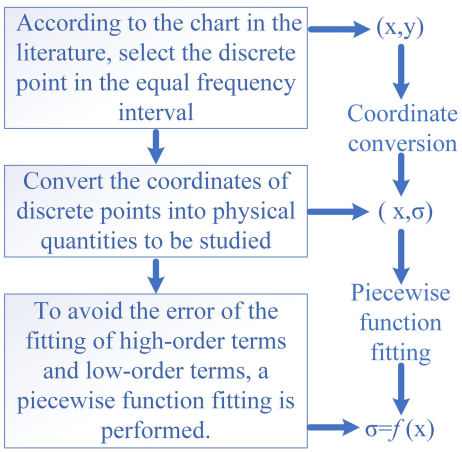

FIGURE 7. Image of the piecewise function fitting process.

The final piecewise function formula is (23), as shown at the bottom of the next page.

B. IMAGE SIMULATION OF THE FULL FREQUENCY RANGE

1) DISTORTED OUTPUT IMAGE DISTURBED BY VIBRATION

Compared with the classic static imaging with a single attitude angle, the ground resolution of the dynamic scanning

mirror imaging changes all the time during the on-orbit scanning. If the sub-satellite point is used as the initial position, the approximate trapezoidal image obtained by the camera on the ground will be enlarged as the swing angle θ increases. When the ground image information is reintegrated in the focal plane, there will be uneven compression between the pixels, which will eventually cause the output image to be distorted. The degree of image distortion becomes deeper as the swing angle θ increases. The earth curvature mapping function $T\{G(x, y)\}$ established by (10) to (13) is used to convert the two-dimensional images of the 6 group imaging models shown in Table 1 with swing angles of 0°, 15°, 30°, 40°, 45°, and 50°. The output images of different attitude angles are shown in Fig.7:

Practically, platform vibration occurs randomly and continuously. When satellites are disturbed by extremely low frequency and extremely large amplitude vibrations, increasing the swing angle θ leads to a longer exposure time of the camera, which in turn introduces more displacement to the focal plane of the camera and reduces the quality of the image. After the above-mentioned distorted image is filtered, it is possible to intuitively compare the degree of degradation of the output image which is disturbed by the superposition of earth curvature distortion and platform vibration. Because the effect of vibration on the pitch axis and the roll axis is the same, the process of degrading the image quality is realized by the product $MTF = \prod_{i=1}^{n} MTF_i(\nu)$ of the two transfer functions, and the formula for the image filtering template is:

$$MTF = \frac{\sin(\pi \cdot d_{avg} \cdot \nu_x)}{\pi \cdot d_{avg} \cdot \nu_x} \times \frac{\sin(\pi \cdot d_{avg} \cdot \nu_y)}{\pi \cdot d_{avg} \cdot \nu_y} \tag{24}$$

The mechanism of the vibration source with a frequency lower than 10Hz is complicated and the amplitude is extremely large. Firstly, (23) can be used to calculate the amplitude of the vibration frequency of 1Hz∼2Hz, and secondly, the equivalent displacement d_{avg} of different attitude angles in the focal plane can be calculated by (18), Finally, the three-dimensional image of the transfer function and the two-dimensional filter template as shown in Fig. 9 are obtained by (24):

Fig.9-(b) shows the transfer function filter template with an attitude angle of 50°. Similarly, the transfer function filter template with an attitude angle of 0°, 15°, 30°, 40°, and 45° can be calculated. Fig.8 is used as the input image of the filtering link, and finally an output image disturbed by vibration as shown in Fig.10 can be obtained.

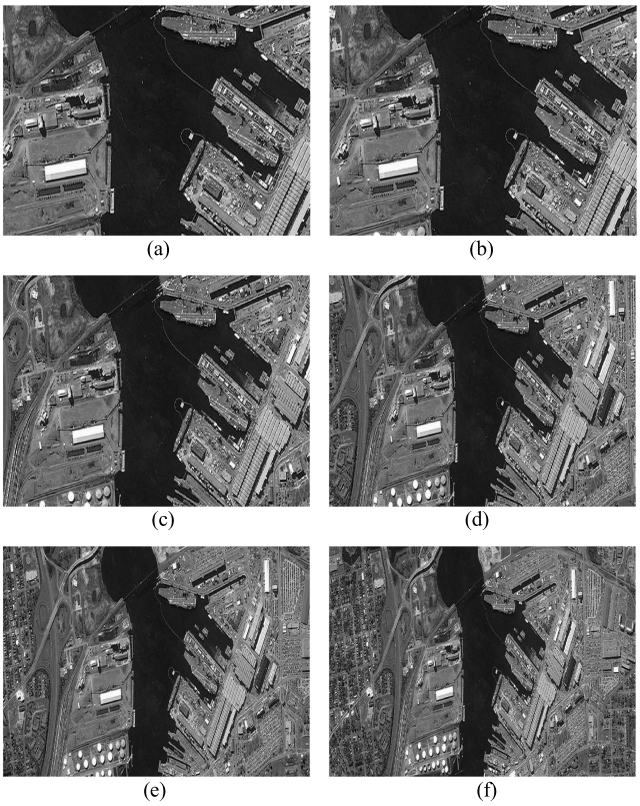

FIGURE 8. Output distortion image of focal plane. (a) output image of 0°; (b) output image of 15°; (c) output image of 30°; (d) output image of 40°; (e) output image of 45°; (f) output image of 50°.

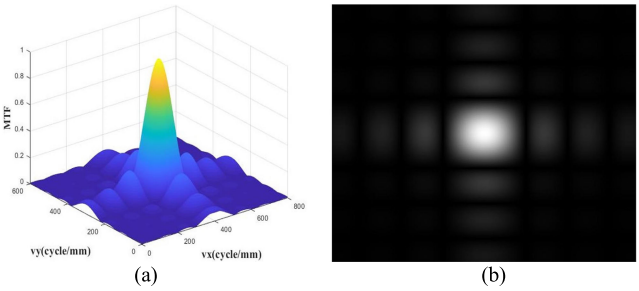

FIGURE 9. Schematic diagram of the transfer function with a swing angle of 50°. (a) Three-dimensional image of transfer function; (b) Two-dimensional image filter template.

$$\sigma = \begin{cases} -0.18x^4 + 2.26x^3 + 6.06x^2 - 158.23x + 479.26 & 0 < \Omega \le 10 \\ \left(1.83 \times 10^{-10}\right)x^7 - \left(6.89 \times 10^{-8}\right)x^6 + \left(1.04 \times 10^{-5}\right)x^5 & \\ \quad - \left(7.88 \times 10^{-4}\right)x^4 - 0.03x^3 + 0.65x^2 - 5.81x - 7.63 & 10 < \Omega \le 100 \\ \left(2.53 \times 10^{-8}\right)x^5 - \left(1.84 \times 10^{-5}\right)x^4 + 0.01x^3 & \\ \quad -0.0.74x^2 + 51.21x - 1386.49 & 100 < \Omega \le 200 \\ 0.1 & 200 < \Omega \le 1000 \end{cases} \tag{23}$$

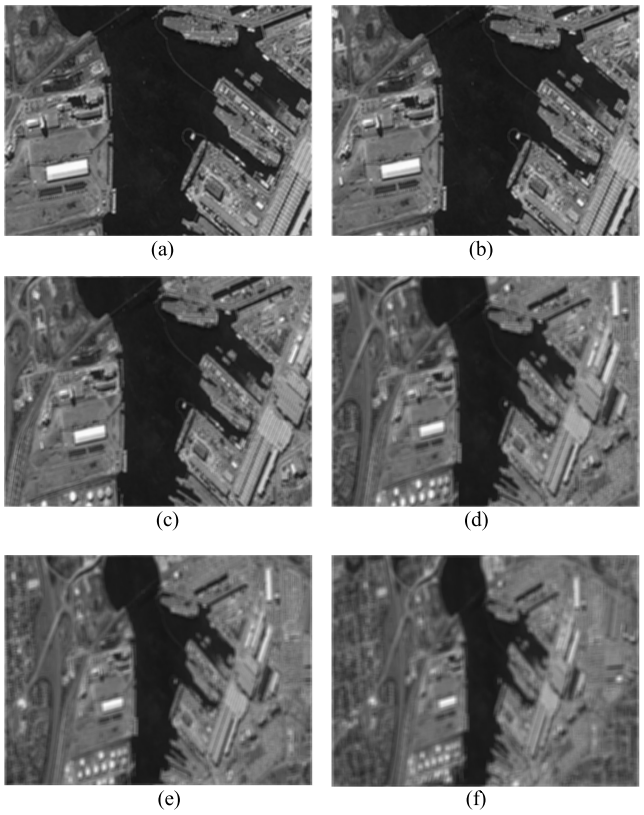

FIGURE 10. Image disturbed by vibration. (a) Degraded image of 0°; (b) Degraded image of 15°; (c) Degraded image of 30°; (d) Degraded image of 40°; (e) Degraded image of 45°; (f) Degraded image of 50°.

In Fig.10, when the attitude angle is 0°, the structure similarity (SSIM) of the filtered output image is 0.58, and the mean square error (MSE) is 53.59. When the attitude angle is 50°, the structure similarity (SSIM) drops to 0.23, the mean square error (MSE) rose to 82.01, which shows that when the platform vibration frequency is extremely low, the increased swing angle will cause the image quality to decrease.

2) ANALYSIS OF VIBRATION DATA EXTRACTED FROM SATELLITE POWER SPECTRAL DENSITY

When analyzing the interference effect of vibration in the whole frequency range on the dynamic scanning mirror imaging system, the transfer function can be used as an index to evaluate the optical system performance. The piecewise function of the amplitude in the full frequency range extracted by the satellite power spectral density is shown in (23), and then transfer function is assigned by the amplitude calculation result, finally a function curve representing the regularity of image quality degradation is obtained.

The camera exposure frequency has always been used as the threshold frequency to distinguish vibration attributes [20], which divides the vibration of the optical platform into low frequency vibration and high frequency vibration. Table 1 lists six groups of instantaneous imaging models with different attitude angles during the imaging process of the dynamic scanning mirror. Due to the different attitude angles of the cameras, the camera exposure frequency gradually increased from 110Hz to 196Hz. Therefore, for these imaging models, platform vibrations with a frequency lower than 110Hz are low frequency vibrations; vibrations with a frequency greater than 196Hz are high frequency vibrations; however, vibrations with frequencies between 110Hz and 196Hz cannot be classified as high or low frequency vibration. At this time, the vibration frequency range is dynamically shifted, and the low frequency vibration is gradually converted to high frequency vibration. In order to simulate the dynamic imaging process disturbed by vibration in the full frequency range, the spatial frequency is taken as the Nyquist frequency $\nu = 1/2a$, a is the pixel size, and the transfer function (19) can be transformed into:

$$MTF\ (\nu) = \begin{cases} \mathrm{J}_0\left(2\pi D/2a\right) & (t \geq T) \\ \mathrm{sinc}\left(\pi d_{avg}/2a\right) & (t < T) \end{cases} \tag{25}$$

The displacement of the focal plane caused by vibration in the frequency range of 10Hz∼100Hz and 100Hz∼200Hz in the (23) is substituted into the transfer function (25), and the transfer function curves as shown in Fig. 11 and Fig. 12 are obtained.

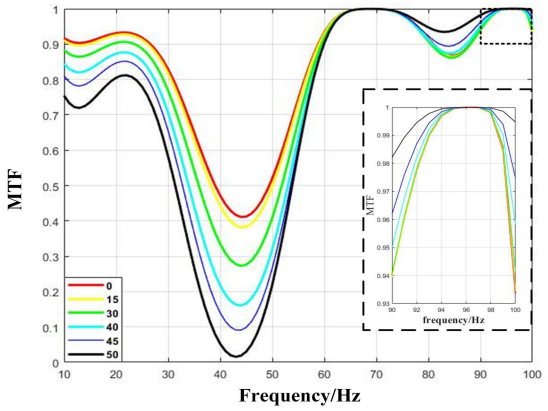

FIGURE 11. MTF from 10Hz to 100Hz.

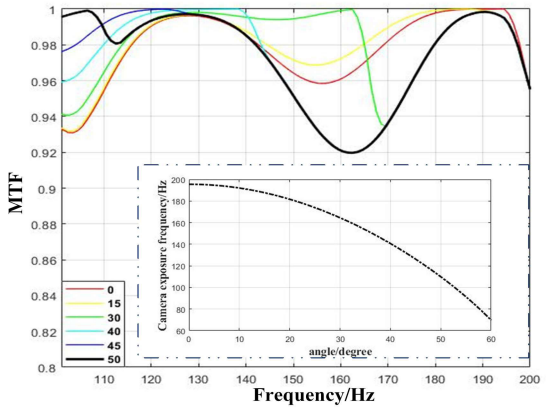

FIGURE 12. MTF from 100Hz to 200Hz.

Fig.11 shows the low frequency vibration transfer function curve with a frequency of 10 Hz to 100 Hz. The low frequency

vibration has a large amplitude and a long vibration period, however the camera's integral time is limited, the focal plane displacement during the camera exposure time is small. Due to the different exposure times of cameras with different attitude angles, the displacement of the camera focal plane caused by vibrations of the same frequency and amplitude is also different, each transfer function curve has independent regularity. When the vibration frequency is lower than 10 Hz, the transfer function of the attitude angle of 0° is better than the transfer function of the attitude angle of 50°, which is the same as the conclusion in the previous section. The transfer function image with a frequency range of 90Hz to 100Hz is partially enlarged. The transfer function of the 50° attitude angle is higher than the transfer function of the 0° attitude angle, which is found to be the opposite of the regularity of the image quality degradation described above. The reason for the above phenomenon is that the scanning motion causes the continuous change of the camera's exposure time, which causes the difference in the displacement of the camera's focal plane. So, before the camera exposure time t_e reaches the half vibration period T/2, the focal plane displacement d_{avg} increases with the increase of the exposure time; after the camera exposure time reaches the half vibration period T/2, the focal plane displacement d_{avg} reduces with the increase of the exposure time. The exposure time of the camera with an attitude angle of 0° is 0.0051 seconds, the vibration period of the platform that most affects the image quality is 0.0102 seconds, and the frequency is 98 Hz; The exposure time of the camera with an attitude angle of 50° is 0.0091 seconds, the vibration period of the platform that most affects the image quality is 0.0182 seconds, and the frequency is 55 Hz. Therefore, in this vibration mode, the intersection of the two transfer function curves is between 55 Hz and 98 Hz.

Fig.12 shows the fitted image of the transfer function with a vibration frequency of 100Hz∼200Hz, and the subgraph shows the camera exposure frequency corresponding to different attitude angles. As the picture shows, the platform vibration changes from low frequency vibration to high frequency vibration with the camera exposure frequency as the threshold. Because the focal plane displacement of high frequency vibration depends on the amplitude of the platform vibration, the transfer function finally converges into a function curve.

Comparing Fig.11 and Fig.12, it can be seen that the amplitude of low frequency vibration is relatively large. The optical platform has a continuous vibration peak in the frequency range of 40Hz to 50Hz, which makes the transfer function drop rapidly, in the fact, the exposure time of the camera limits the displacement of the camera's focal plane. The amplitude of high frequency vibration is relatively small, but the camera exposure time is relatively long. When the vibration frequency is close to the imaging line frequency, the displacement of the focal plane of the camera increases, Therefore, the transfer function of platform vibration drops rapidly during the transition from low frequency vibration to high frequency vibration. Different from the classic static imaging, the camera exposure time of the dynamic scanning mirror imaging mode is diversified, so the high and low frequency vibration types will replace each other, and there will be a situation where the amplitude is extremely large and the exposure time is extremely long. At this time, there are two interference factors superimposed on the imaging system which have a great impact on the output image.

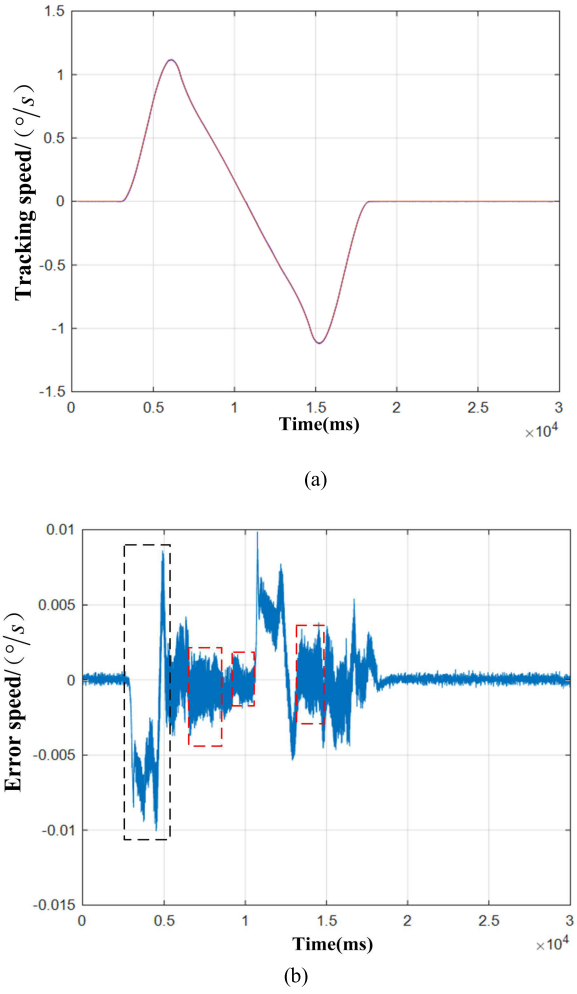

FIGURE 13. Ground test output image. (a) Speed tracking curve; (b) Speed tracking error.

3) ANALYSIS OF VIBRATION DATA TESTED ON GROUND PLATFORM

Fig.13-(a) shows the speed tracking curve measured by the ground optical platform test center, and Fig.13-(b) shows the speed error caused by vibration. The black dotted area represents the long-period vibration. Actually, a single period of vibration is difficult to clarify the regularity of image degradation; The red dashed area indicates vibrations that occur repeatedly with the same amplitude and frequency, and the conclusion of the image degradation simulation can be illustrated by using this part of the vibration as the investigation variable.

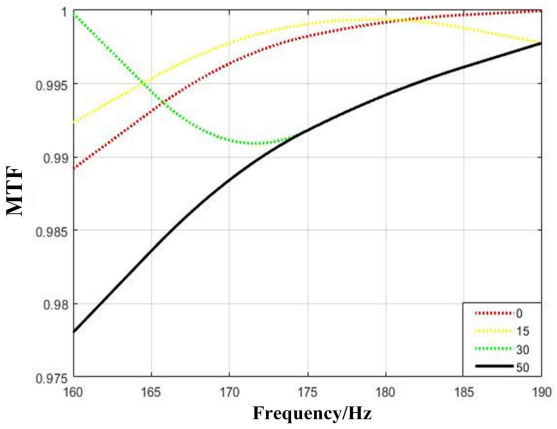

FIGURE 14. MTF for ground testing.

The selected vibration frequency range is 160Hz∼190Hz, and the MTF curve is shown in Fig.14. By comparing Fig.12 and Fig.14, it can be seen that the satellite power spectral density is the average value of multiple satellites. Although the platform test data and the general data extracted by the satellite power spectral density are different to a certain extent, the transfer function decline law of the two sets of data is similar, which can be consistent with the simulation conclusions.

4) ANALYSIS OF HIGH FREQUENCY VIBRATION

In the above six groups of motion models, platform vibrations with a frequency greater than 200 Hz are all high frequency vibrations, and the attitude angle hardly affects high frequency vibrations. It is well known that when the MTF of the remote sensing image is lower than 5%, it hardly affects the further analysis of the image. Fig.15 shows the transfer function curve of high frequency vibration not less than 95%, where the abscissa is the focal plane displacement, and the ordinate is the transfer function value. If the MTF drops by 5%, the image displacement will be 7.89×10^{-4}mm, the deflection angle of the optical axis calculated by (17) is 0.79μrad.

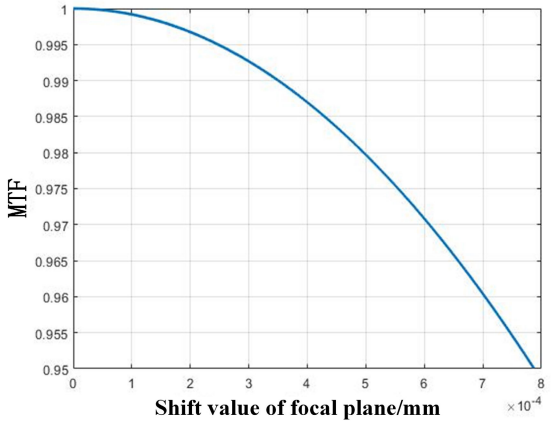

FIGURE 15. MTF of high frequency.

5) CONCLUSION OF IMAGE SIMULATION

Section III discusses the impact of multisource vibration on the output image of the system in the dynamic scanning mirror imaging mode. The scanning speed of the camera is set to 10°/s, and the instantaneous imaging model is established with attitude angles of 0°, 15°, 30°, 40°, 45° and 50°. The simulation conclusions are summarized as follows:

1) In the process of dynamic scanning mirror imaging, the camera attitude angle θ is a periodic function $\theta(t)$ of time, and the camera attitude angle affects the camera imaging integration time. If the imaging time of the sub-satellite point is taken as the initial time, the camera exposure time will increase as the swing angle increases (within the maximum imaging range).

2) When the vibration frequency is extremely low, as the camera attitude angle θ increases, the level of distortion of the image is increased, and the quality of the remote sensing image becomes worse. Compared with other models, the imaging model with a posture angle of 50° has the largest amount of information in the output image of the camera focal plane. The attitude angle increases from 0° to 50°, the camera exposure time is extended, and the output image structure similarity (SSIM) is reduced by 0.35, mean square error (MSE) increased by 28.42, and the image was significantly degraded.

3) Combining the satellite power spectrum density analysis of the image degradation phenomenon disturbed by the vibration of the full frequency range, it can be seen that the low frequency vibration transfer function of different attitude angles is different and has independent regularity. The platform vibration changes from low frequency vibration to high frequency vibration with the camera exposure frequency as the critical value, and the function converges into a curve. The reason for the above phenomenon is that the equivalent displacement of the focal plane during the exposure time of the camera at different attitude angles is different, resulting in a certain difference in the regularity of the image quality degradation. Under high frequency vibration, the camera exposure time is no longer an important factor affecting the displacement of the focal plane, so the impact on image quality is low, and the transfer function tends to be consistent.

4) The focal plane displacement of high frequency vibration is twice the vibration amplitude. Taking imaging requirements as constraints, the maximum focal plane displacement and displacement angle that do not affect the high-quality of output images can be calculated. For the dynamic imaging model that has been constructed, when the deviation angle of the optical axis is less than 0.79μrad, it meets the imaging requirements.

IV. CONCLUSION

Based on the motion principle of scanning mirror imaging, a ground scene curvature mapping function based on scanning motion equations and an image quality degradation model fused with vibration source filter templates are

established, respectively. Combined with satellite power spectral density, the nonlinear least squares method is used to obtain the function of vibration source with respect to amplitude and frequency, and the degradation process of multisource vibration image of scanning imaging is simulated.

During the scanning mirror imaging of the space-based payload ground scene, the image resolution decreases as the attitude angle increases, and the image quality is hardly affected; However, the multisource vibration of scanning imaging has a certain effect. Low-frequency vibration with large amplitude will cause distortion and deterioration of the output image. Simultaneously, due to the scanning movement of the swing mirror, the exposure frequency changes, and the frequency critical point of the vibration type conversion makes an increase to the frequency critical interval; High-frequency vibrations approaching the imaging line frequency directly interfere with image quality, at this time, the imaging quality decreases rapidly as the amplitude increases. In summary, it is necessary to effectively suppress platform vibration with large amplitude and high frequency. This article expects to have a certain significance for image quality degradation suppression and image quality evaluation of space-based scanning imaging.

REFERENCES

[1] J. Keller, "Delivering weapons and sensor payloads from future large unmanned submarines," *Mil. Aerosp. Electron.*, vol. 30, no. 7, pp. 8–11, 2019.
[2] S. K. Dhakad, U. Dwivedi, and S. Baudha, "Performance improvement of fractal antenna with electromagnetic band gap (EBG) and defected ground structure for wireless communication," in *Optical and Microwave Technologies* (Lecture Notes in Electrical Engineering), vol. 468, G. Gnanagurunathan, R. Sangeetha, and K. Kiran, Eds. Singapore: Springer, 2018, pp. 9–19.
[3] K. C. A. Kumar, G. P. O. Reddy, P. Masilamani, S. Y. Turkar, and P. Sandeep, "Integrated drought monitoring index: A tool to monitor agricultural drought by using time-series datasets of space-based earth observation satellites," *Adv. Space Res.*, vol. 67, no. 1, pp. 298–315, Jan. 2021.
[4] C. Wang, H. D. Shi, and Y. C. Li, "Design of super-resolution telescopic imaging optical system with relative large field-of-view," *Acta Optic sinica*, vol. 40, no. 13, pp. 153–162, 2020.
[5] J. Y. Li, W. X. Feng, and F. Liu, "Design of airborne multi-scale wide-field-of-view and high-resolution imaging system," *Acta Optic sinica*, vol. 41, no. 2, pp. 50–60, 2021.
[6] T. Xu, X. Yang, S. Wang, J. Han, L. Chang, and W. Yue, "Imaging velocity fields analysis of space camera for dynamic circular scanning," *IEEE Access*, vol. 8, pp. 191574–191585, 2020.
[7] X. B. Yang, J. Q. Wang, and G. Jin, "Calculation of line frequency for rotational pendulum imaging of the TDI camera vertical track," Chin. Patent 107 702 697 B, Nov. 29, 2019.
[8] Y. Yuan, J. Qiu, and Z. L. Wang, "Study on design of scanning mirror system for area array imaging," *Aerosp. Shanghai*, vol. 33, no. 6, pp. 72–77, 2016.
[9] W. Xu, G. Jin, and J. Wang, "Optical imaging technology of JL-1 lightweight high resolution multispectral remote sensing satellite," *Opt. Precis. Eng.*, vol. 25, no. 8, pp. 1969–1978, 2017.
[10] X. Zhai, Y. Luo, Y. Zhang, and S. Xie, "Fuzzy PD hybrid control of low frequency vibration of annular antenna," *Proc. Inst. Mech. Eng., G, J. Aerosp. Eng.*, vol. 235, no. 6, pp. 718–726, May 2021.
[11] W. A. Wahballah, F. Eltohamy, and T. M. Bazan, "Influence of attitude parameters on image quality of very high-resolution satellite telescopes," *IEEE Trans. Aerosp. Electron. Syst.*, vol. 57, no. 2, pp. 1177–1183, Apr. 2021.
[12] H. Q. Liu, H. M. Ma, and Z. H. Jiang, "Algorithm for satellite-platform jitter estimation in period of non-overlapping images," *Acta Opt. Sinica*, vol. 39, no. 5, pp. 169–180, 2019.
[13] M. Toyoshima, Y. Takayama, and H. Kunimori, "In-orbit measurements of spacecraft microvibrations for satellite laser communication links," *Opt. Eng.*, vol. 49, no. 8, p. 578, 2010.
[14] O. Hadar, I. Dror, and N. S. Kopeika, "Image resolution limits resulting from mechanical vibrations. Part IV: Real-time numerical calculation of optical transfer functions and experimental verification," *Opt. Eng.*, vol. 33, no. 2, pp. 566–578, 1994.
[15] S. Chen, M. Xuan, J. Xin, Y. Liu, S. Gu, J. Li, and L. Zhang, "Design and experiment of dual micro-vibration isolation system for optical satellite flywheel," *Int. J. Mech. Sci.*, vol. 179, Aug. 2020, Art. no. 105592.
[16] Z. Wang, *Platform Jitter Effect on Image Quality of Spaceborne TDICCD Camera*. Changchun, China: Changchun Institute of Optics, 2014.
[17] J. H. Wei, *Imageing Modeling and Image Simulation of Space-Based Measurement Camera*. Harbin, China: Institute of Technology, 2017.
[18] S. W. Pang, Q. R. Guo, and W. He, "Influence of micro-vibration on image quality of a remote sensing satellite," *Spacecraft Environ. Eng.*, vol. 36, no. 1, pp. 47–55, 2019.
[19] J. Sudey and J. R. Schulman, "In-orbit measurements of Landsat-4 thematic mapper dynamic disturbances," *Acta Astronautica*, vol. 12, nos. 7–8, pp. 485–503, Jul. 1985.
[20] J. F. Shi, P. F. Cheng, and H. Yuan, "Analysis and verification of effect of micro-vibration on space photoelectric payload imaging," *Acta Opt. Sinica*, vol. 39, no. 5, pp. 277–283, 2019.

ZIQI YU received the B.S. degree from Tonghua Normal University, Tonghua, China, in 2019. He is currently pursuing the M.S. degree with the College of Science, Changchun University of Science and Technology. His research interests include space optical remote sensing imaging simulation and satellite platform vibration analysis.

LI JIANG received the B.S. degree in physics and the Ph.D. degree in optical engineering from Jilin University, Changchun, China, in 2006 and 2011, respectively. From 2011 to 2017, she was a Lecturer with the College of Science, Changchun University of Science and Technology, China. Since 2018, she has been an Associate Professor with the College of Science, Changchun University of Science and Technology. Her research interests include dynamic target-tracked imaging by space-based payload and the imaging simulation of space optical remote sensing.

ZHIHAI YAO received the B.S. and Ph.D. degrees in physics from Changchun University of Science and Technology, Changchun, China, in 1988 and 2007, respectively. He is currently a Professor with the College of Science, Changchun University of Science and Technology. His research interests include nonlinear optics, theory, and computational physics.